Supramolecular Chemistry
Publication details, including instructions for authors and subscription information:
http://www.informaworld.com/smpp/title~content=t713649759

Synthesis and Enantioselective Recognition of a Calix[5]arene-based Chiral Receptor

Takeharu Haino[a]; Hiroyuki Fukuoka[a]; Hajime Iwamoto[a]; Yoshimasa Fukazawa[a]
[a] Department of Chemistry, Graduate School of Science, Hiroshima University, Higashi-Hiroshima, Japan

To cite this Article Haino, Takeharu , Fukuoka, Hiroyuki , Iwamoto, Hajime and Fukazawa, Yoshimasa(2008) 'Synthesis and Enantioselective Recognition of a Calix[5]arene-based Chiral Receptor', Supramolecular Chemistry, 20: 1, 51 — 57
To link to this Article: DOI: 10.1080/10610270701742553
URL: http://dx.doi.org/10.1080/10610270701742553

Supramolecular Chemistry, January–March 2008 Vol. 20 (1–2), pp. 51–57

Synthesis and Enantioselective Recognition of a Calix[5]arene-based Chiral Receptor

TAKEHARU HAINO*, HIROYUKI FUKUOKA, HAJIME IWAMOTO and YOSHIMASA FUKAZAWA

Department of Chemistry, Graduate School of Science, Hiroshima University, 1-3-1, Kagamiyama, Higashi-Hiroshima 739-8526, Japan

(Received 2 August 2002; Accepted 11 October 2007)

Dedicated to Prof. David N. Reinhoudt

Calix[5]arene-based artificial receptor 1 capped with chiral macrocycle 6 was synthesized and showed strong binding towards ethyltrimethylammonium derivatives via cation/π and/or hydrogen bonding interactions. The calix[5]arene cavity provided the dissymmetric guest-binding environment in which chiral guests 9–19 were encapsulated in an enantioselective fashion. Thermodynamic studies for this chiral recognition gave an insight into the binding manner of the receptor: the enantioselective recognition is enthalpy favoured. Probably, the attractive interactions between the host and the guest gives rise to the enthalpy difference in enantioselection; however, the enthalpy gains of one of the enantiomers are compensated by entropy costs, reducing the enantioselectivity of the receptor.

Keywords: Calix[5]arene; Chiral recognition; Chiral trimethylammonium; Cavity; Cation/π

INTRODUCTION

Chiral recognition is a key event in nature. Many enzymes and receptors produce their biological functions by discriminating the chiral centre on substrates, the efficiency of which depends upon a chiral moiety. To achieve efficient enantioselectivity, they take advantage of many noncovalent interactions: hydrogen bonding, van der Waals, solvophobic, dipole–dipole, CH/π, cation/π, etc. [1]. Chiral substrates create many noncovalent interactions with chiral entities placed inside their binding pockets, one enantiomer binding more strongly than its antipode.

Chiral recognition is a long-standing issue in the field of supramolecular chemistry [2]. It involves preferred recognition of an enantiomeric molecule out of its racemic mixtures. Discrimination of a chiral centre of a molecule imposes an additional constraint on a suitable platform, creating an effective chiral environment, compared with achiral molecular recognition. Much effort has been devoted to employing steric and electronic interactions to create a chiral environment in which one component of the racemic mixture can be preferentially bound.

Chiral crown ethers are fascinating developments in the field of supramolecular chemistry [3]. Chiral biaryl units were directly incorporated into a crown ring, creating a chiral-binding environment. The enantiomers of chiral ammonium salts showed preferential binding over their antipodes. Incorporation of multipoint recognition sites onto a receptor produces a high enantioselectivity. For instance, de Mendoza and co-workers have reported a guanidinium salt having crown and aromatic moieties, which showed good enantioselectivity to amino acids via π–π stacking, and hydrogen bonding to both the crown and the guanidinium units [4]. Still and co-workers have shown C_3-symmetric macrocyclic and two-armed receptors [5]. These receptors have many hydrogen bonding groups placed inside the guest-binding space, bringing about high enantioselective binding via hydrogen bonding interactions. Recently, simple chiral C_3-receptors have been created, presenting enantioselective guest selection [6].

*Corresponding author. E-mail: haino@sci.hiroshima-u.ac.jp

ISSN 1061-0278 print/ISSN 1029-0478 online © 2008 Taylor & Francis
DOI: 10.1080/10610270701742553

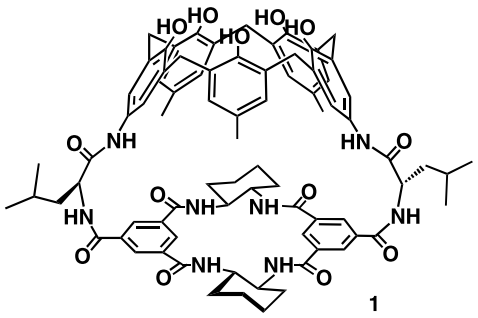

FIGURE 1 Chiral receptor **1** based on a calix[5]arene.

One of the most popular platforms to build up a chiral guest-binding environment is the calixarene family. Chiral receptors based on a calix[4]arene have been developed to functionalise their upper or lower rims [7]. However, calix[5]arene-based chiral receptors are limited so far, although, it has a larger cavity capable of capturing a sizable guest. We have continuously studied calix[5]arene-based artificial receptors, capable of taking up a guest molecule into its cavity through noncovalent interactions: van der Waals, CH/π, etc. [8]. In this paper, we present chiral calix[5]arene-based receptor **1** equipped with chiral macrocycle **6** [9] of isophthalic acid and (1*S*, 2*S*)-*trans*-1,2-diaminocyclohexane (Fig. 1).

The chiral macrocyclic ring provides the additional constraint to produce the dissymmetric guest-binding space in the calix[5]arene cavity. The four amide N—H protons of the macrocyclic ring are inwardly oriented to create the multipoint hydrogen bonding interactions with a guest having a polar functionality, and the π-basic aromatic cavity of the calix[5]arene can allow a cationic guest to be accommodated in it via interactions such as van der Waals, cation/π, CH/π, etc. If a chiral guest has cationic and hydrogen bonding functionalities, it can take advantage of the noncovalent interactions to be accommodated inside the cavity of the receptor.

RESULTS AND DISCUSSION

Synthesis of **1** started from the known calix[5]arene **2** (Scheme 1) [10]. Diazo coupling of **2** with 4-carboxybenzenediazonium nitrate worked well to give the bis(4-carboxyazo)calix[5]arene as a precipitate. Subsequent reduction of the N═N double bonds produced diamino calix[5]arene **3** [11]. The coupling reaction of **3** and *N*-*t*-butyloxycarbonyl-L-leucine with 1-ethyl-3-(3′-dimethylaminopropyl)carbodiimide and 1-hydroxy-7-azabenzotriazole in dichloromethane proceeded at 40°C to give **3** in 38% yield. Treatment of **3** with trifluoroacetic acid in dichloromethane gave ammonium salt **5** in 86% yield. The coupling reaction of **5** with **6** in the presence of diisopropylethylamine at 60°C in dimethylformamide furnished the desired host **1** in 32% yield.

Chemical structures of all the guests used in the binding studies with **1** are shown in Fig. 2. The complexation behaviour of achiral guest **7** with **1** was studied in order to gain an insight into its binding manner. A titration experiment of **7** with **1** at 293 K in chloroform was carried out using absorption spectroscopy. An isosbestic point appeared at 464 nm, and Job plots confirmed the 1:1 stoichiometry of the host–guest complex (Fig. 3). The curve-fitting analysis gave an association constant of $K_a = 13{,}000 \pm 1000\,\mathrm{l\,mol^{-1}}$.

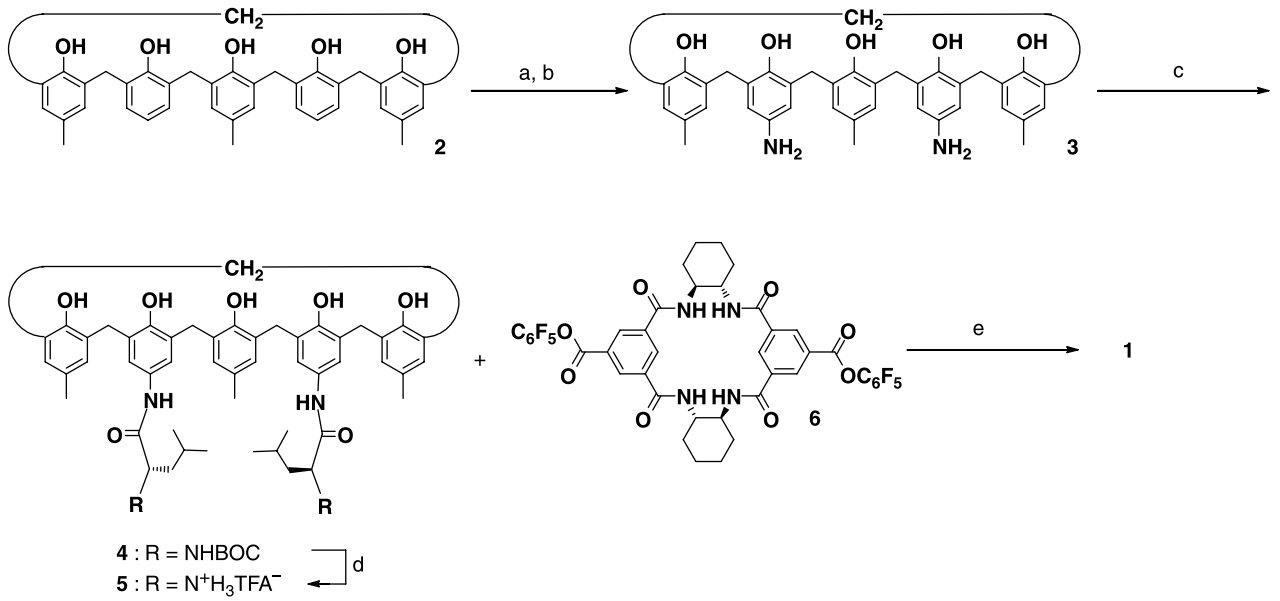

SCHEME 1 Reagents and conditions: (a) *p*-aminobenzoic acid, $NaNO_3$, AcONa/DMF, MeOH, 0°C, 4 h; (b) $Na_2S_2O_4$, 1% NaOH(aq.), 60°C, 2 h, 68%; (c) *N*-BOC-L-leucine, HOAt, EDCI/CH_2Cl_2, RT, 3 h, 38%; (d) TFA/CH_2Cl_2, RT, 1 h, 86%; (e) *i*-Pr_2NEt/DMF, 80°C, 24 h, 32%.

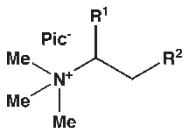

7: R^1 = H, R^2 = OAc 14: R^1 = *i*-Pr, R^2 = OAc
8: R^1 = H, R^2 = OH 15: R^1 = *i*-Pr, R^2 = OH
9: R^1 = Ph, R^2 = H 16: R^1 = *i*-Bu, R^2 = OAc
10: R^1 = Ph, R^2 = OAc 17: R^1 = *i*-Bu, R^2 = OH
11: R^1 = Ph, R^2 = OH 18: R^1 = CH_2Ph, R^2 = OAc
12: R^1 = Me, R^2 = OAc 19: R^1 = CH_2Ph, R^2 = OH
13: R^1 = Me, R^2 = OH

FIGURE 2 Cationic guests.

The decreased values of the protons distant from the nitrogen atom place the acetoxyl group outside the cavity.

The association constants for the guests shown in Fig. 2 were determined by a standard titration technique, as shown with **7** using absorption spectroscopy (Table I). The encapsulation of **9** was driven only by a cation/π interaction to the π-basic

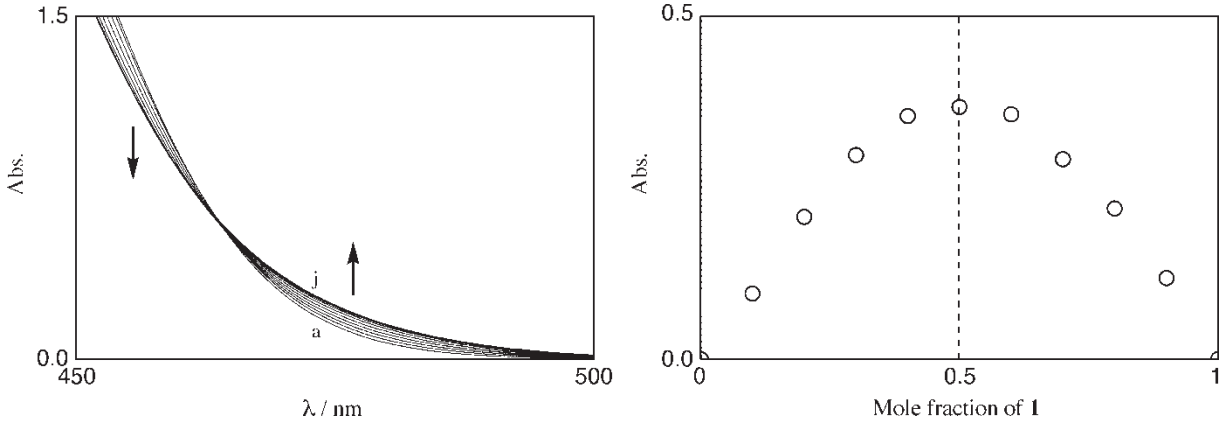

FIGURE 3 The absorption spectra of **7** (4.61×10^{-4} mol L^{-1}) in chloroform upon the addition of **1** (a, 0.0; b, 0.92; c, 1.84; d, 2.77; e, 4.61; f, 5.53; g, 6.45; h, 7.38; i, 8.30; j, 9.22×10^{-4} mol l^{-1}) and Job plot of **7** and **1**.

The structural information of the complex was given by a ^{1}H NMR titration experiment in chloroform-d_1. Upon the addition of **1** to a solution of **7**, significant upfield shifts of the guest protons (Me—N, −2.13; N—CH_2, −2.16; OCH_2, −1.51; C(O)Me, −0.34 ppm) were observed (Fig. 4). Characteristic upfield shifts of the methyl and methylene protons adjacent to the nitrogen atom are more than −2 ppm, indicating that the trimethylammonium group stays deep inside the cavity of the calix[5]arene to create a cation/π interaction [12].

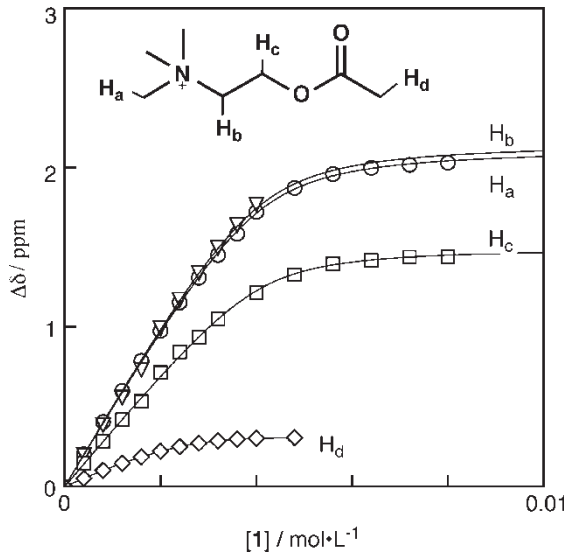

FIGURE 4 Chemical shift changes of the protons of **7** (4.09×10^{-3} mol l^{-1}) upon the addition of **1** in chloroform-d_1.

cavity of **1** in an enantioselective fashion. This indicates that **9** recognized the dissymmetric binding environment of **1** only by noncovalent interactions. Attaching the hydrogen bonding functionalities onto guest **9** increased its binding ability (**9** versus **10** and **11**), suggesting that the newly attached functionalities should form hydrogen bonds to the macrocyclic amides, providing additional stabilization of the host–guest complex. Preferential binding of the ***R***-isomers to **1** was observed for **12**–**19**, except **17**. The 2-hydroxyethyltrimethylammonium salts showed slightly higher selectivity's than the corresponding 2-acetoxy salts. This means that the hydrogen bonding interaction between the host and the guest most likely plays a key role in the chiral discrimination. The enantioselectivity of **1** is not sensitive to the size of the alkyl substituents (**12**–**17**). In contrast, the opposite sense of the enantioselectivity is observed in guests possessing aromatic rings (**10** and **11** versus **18** and **19**), suggesting that just a tiny difference in their structures can lead to discrimination. The highest enantioselectivity is achieved in **19**. This indicates that the aromatic rings play a key role in the enantioselectivity.

To gain an insight into the structure of the host–guest complex with chiral guest **15**, the complexation-induced shift changes of the guest protons were measured (Fig. 5). The guest protons (H_a, H_b and H_c) appeared at 2.35, 1.19 and 1.13 ppm, respectively, without **1** in chlororform-d_1. In both isomers, these protons moved in the clear window above 0.0 ppm, and their complexation-induced upfield shifts were

TABLE I Association constants (K_a/1 mol^{-1}) of **1** for **7**–**19** at 293 K in chloroform

Guest	K_a	*R*:*S*	Guest	K_a	*R*:*S*
7	13,000 ± 1000		***R*-14**	17,000 ± 2000	1.9:1.0
8	14,000 ± 1000		***S*-14**	9000 ± 1000	
***R*-9**	2400 ± 100	1.0:2.0	***R*-15**	21,000 ± 1000	2.4:1.0
***S*-9**	4900 ± 200		***S*-15**	8600 ± 800	
***R*-10**	9800 ± 1000	1.0:1.5	***R*-16**	4300 ± 500	2.2:1.0
***S*-10**	15,000 ± 2000		***S*-16**	2000 ± 300	
***R*-11**	12,000 ± 1000	1.0:1.4	***R*-17**	6700 ± 500	1.0:1.2
***S*-11**	17,000 ± 2000		***S*-17**	7800 ± 800	
***R*-12**	20,000 ± 1000	2.0:1.0	***R*-18**	32,000 ± 5000	1.6:1.0
***S*-12**	10,100 ± 800		***S*-18**	20,000 ± 2000	
***R*-13**	4700 ± 200	2.2:1.0	***R*-19**	26,000 ± 3000	3.7:1.0
***S*-13**	2100 ± 200		***S*-19**	7100 ± 900	

more than −2 ppm, indicating that the protons stayed in the highly shielded region of the five phenolic rings of the calix[5]arene.

Molecular mechanics calculations on the complexes of **1** with ***R*-15** nd ***S*-15** were carried out with MacroModel V.9.1 using the OPLS2005 force field, together with the GB/SA solvation parameters for $CHCl_3$ [13]. In the complex structure of **1** and **15**, the guest hydroxyl group forms a hydrogen bond to one of the carbonyl groups of the macrocyclic amide (Fig. 6). The trimethylammonium and the isopropyl groups stay deep inside the calix[5]arene cavity, facing towards the phenolic rings. The calculated structures of the host–guest complex rationalized that the host–guest complexation brought about the large upfield shifts of the proton signals of the isopropyl groups upon complexation. Apparently, the steric interaction between the isopropyl group and the aromatic rings should drive the enantioselective binding of the guest within the dissymmetric cavity of the host.

To obtain information on the host–guest association, thermodynamic parameters for the complexation of the selected guests were determined using van't Hoff plots (Table II). Comparison of the relative enthalpic and entropic components of the complexes of **1** with the guests provides for a more detailed picture of the driving forces for their encapsulation (Table II). The complexation of the guests gave rise to the negative enthalpic components for the complexation, undoubtedly composed of a variety of noncovalent interactions:cation/π, van der Waals and hydrogen bonding. Although, the free energy change for the complexation of achiral guest **7** is close to that of **8**, the complexation of **8** brought about a much larger enthalpic component than that of **7** ($\Delta H = 14.8$ kcal mol^{-1}). This suggests that the hydroxyl group of **8** should form hydrogen bonds

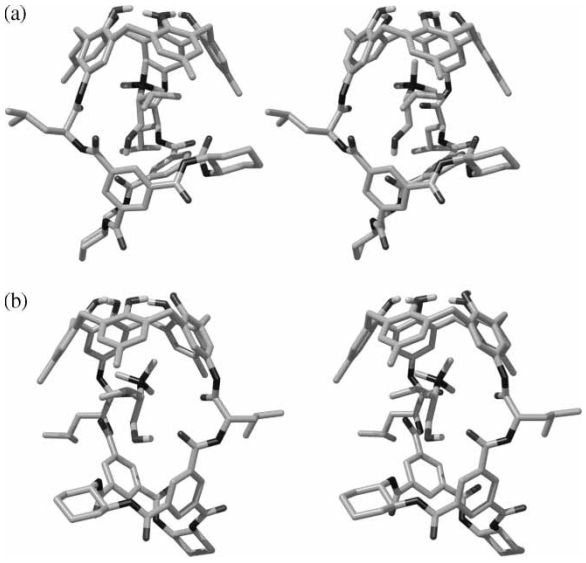

FIGURE 6 Stereoplots of the calculated complex structures of **1** with (a) ***R*-15** and (b) ***S*-15**.

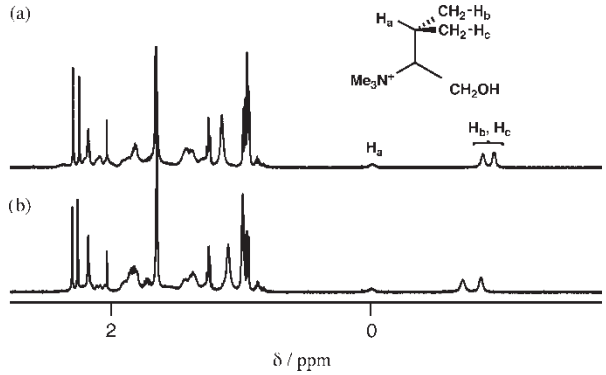

FIGURE 5 ^{1}H NMR spectra of (a) ***R*-15** and (b) ***S*-15** (2.0×10^{-3} mol l^{-1}) with 1.5 equiv. of **1** in chloroform-d_1.

TABLE II Thermodynamic parameters of the host–guest complexes with the selected guests

Guest	$\Delta G_{293\,K}$ (kcal mol^{-1})	ΔH (kcal mol^{-1})	ΔS (cal K^{-1} mol^{-1})
7	−5.55	−4.9	+2.2
8	−5.42	−19.7	−48.7
***R*-11**	−5.73	−9.3	−11.9
***S*-11**	−6.40	−15.4	−30.7
***R*-15**	−5.85	−13.5	−26.1
***S*-15**	−5.47	−10.6	−17.5
***R*-17**	−5.22	−12.4	−24.5
***S*-17**	−5.50	−7.8	−8.0
***R*-19**	−5.79	−21.0	−51.0
***S*-19**	−5.27	−3.9	+4.7

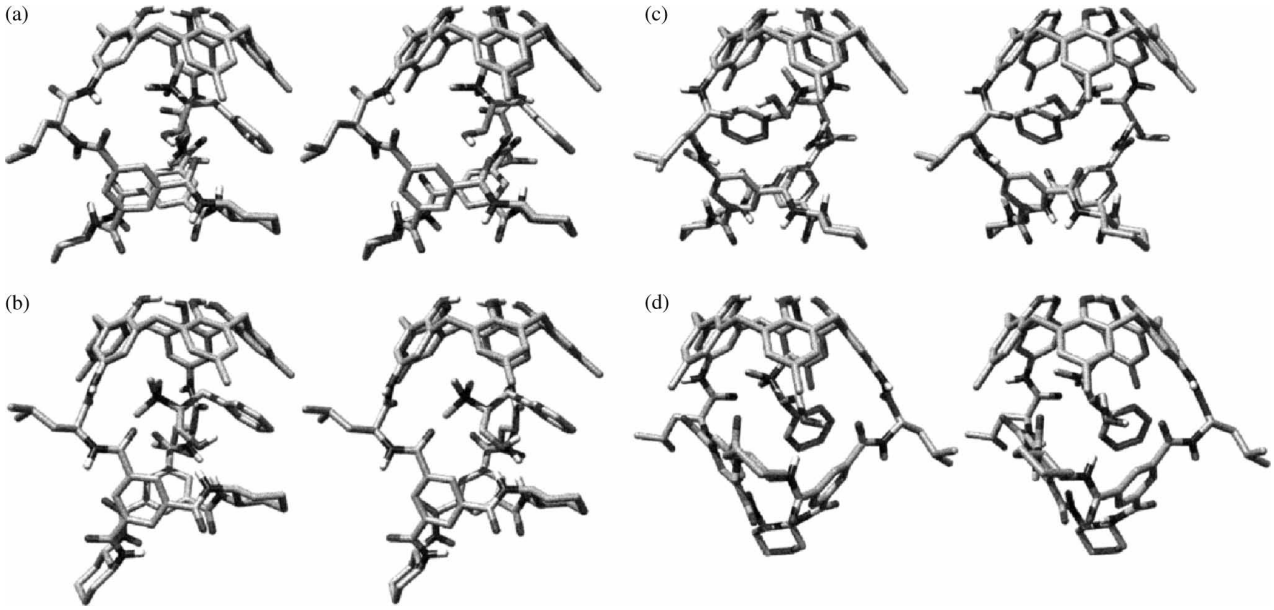

FIGURE 7 Stereoplots of the calculated complex structures of **1** with (a) ***R*-19**, (b) ***S*-19**, (c) ***R*-11** and (d) ***S*-11**.

to the host amides, which are stronger than those of **7**. As a result, **8** has to pay an entropic cost due to the loss of the freedom of the movements in the host cavity; this rationalizes the large negative entropic component ($\Delta S = -48.7\,\text{cal}\,\text{K}^{-1}\,\text{mol}^{-1}$).

Although, general insights on chiral selectivity in the present system cannot be provided, the enantioselective recognition of **1** with guests (**11**, **15**, **17** and **19**) is mainly driven by the enthalpic contribution, resulting from the noncovalent interactions. It is interesting that the host preferentially recognized the ***S***-isomer over the ***R***-isomer in the complexation of **11**, whereas **19** showed the opposite enantioselectivity even though they show only a small difference: the presence or absence of the methylene next to the phenyl ring. The enthalpy difference between the ***R***- and ***S***-isomers in **19** is $-17.1\,\text{kcal}\,\text{mol}^{-1}$ while that in **11** is only $-6.1\,\text{kcal}\,\text{mol}^{-1}$. This impressive difference between the enthalpies can be rationalized by the contribution of the $\pi-\pi$ stacking interaction. The phenyl ring of **19** adopts a parallel arrangement to one of the phenolic rings of the calix[5]arene in the calculated structure, but that of **11** does not (Fig. 7). This might produce the large enthalpy difference and the opposite selectivity.

The compensation relationship [14] between the enthalpy and entropy changes was observed here with the supramolecular complexations (Table II). Plotting the enthalpies versus the entropies gave a good linear correlation ($R^2 = 0.998$). This shows that the stronger the attractive interaction between the host and the guest, the more reduced the freedom of the guest movement in the supramolecular complex, which results in an entropy loss. Indeed, ***R*-19** receives the largest enthalpy gain during the complexation, but has to pay the largest entropy cost. The enthalpy gain of ***S*-19** with complexation is the smallest, which suggests that the guest still has some freedom of movement in the cavity, which is of course smaller than the available space on the outside of the cavity. In this case, the contribution of the desolvation inside the cavity overcomes the entropy loss due to the restriction of the freedom of the guest's movement in the complex [15]. Accordingly, both the solvation–desolvation and change in the freedom of the guest's movement play important roles in the complex formation in organic media.

CONCLUSION

We have demonstrated the synthesis of a new type of chiral calix[5]arene-based receptor **1** and its interesting enantioselective recognition. Chiral recognition is still an ongoing issue in supramolecular as well as bioorganic chemistries. Although, it is difficult to present the details of the chiral recognition in this system, this new type of chiral receptor should provide another way to create chiral recognition for many chiral substrates. The chiral recognition of the receptor might give rise to a wide range of possible applications, including molecular catalysts and chiral sensors.

EXPERIMENTAL

General Methods

^{1}H NMR spectra were measured with a JEOL ECA-600 or a JEOL Lambda 500 spectrometer using a residual solvent as an internal standard. ^{13}C NMR spectra were taken with a JEOL Lambda 500 or a JEOL ECA-600

spectrometer. ^{13}C NMR chemical shifts (δ) are given in ppm from internal chloroform-*d* ($\delta = 77.0$) and methanol-d_4 ($\delta = 49.0$). IR spectra were measured on a JASCO FT/IR-420S spectrometer. Mass spectra were reported with a JEOL JMX-SX 102 mass spectrometer. Elemental analyses were performed on a Perkin Elmer 2400CHN elemental analyser. Melting points were measured with a Yanagimoto micro-melting point apparatus. UV spectra were measured on a JASCO V-560 spectrometer.

All reactions were carried out under an argon atmosphere unless otherwise noted. Dichloromethane and dimethylformamide were freshly distilled from CaH_2. Column chromatography was performed using Merck silica gel (70–230 mesh). All reagents were of commercial grade and were used without further purification.

Synthesis

5,17-Diamino-11,23,29-trimethyl-31,32,33,34,35-pentahydroxy-Calix[5]arene 3

To a solution of calix[5]arene **2** (700.0 mg, 1.22 mmol), sodium acetate (1.35 g, 16.5 mmol) in DMF (10 ml) and MeOH (6 ml) was added slowly to a solution of 4-aminobenzoic acid (1.25 g, 9.11 mmol) and sodium nitrite (1.15 g, 16.7 mmol) in aqueous HCl (0.67 mol l^{-1}, 45 ml) at 0°C. After being stirred at the same temperature for 6 h, the resulting red suspension was filtrated and the reddish paste was washed with water. The resulting moist paste was dissolved in an aqueous NaOH solution (1%, 300 ml) and sodium hydrosulphite (23.8 g, 136 mmol) was added into the solution. After being stirred at 60°C for 4 h, the resulting suspension was cooled and extracted with $CHCl_3$. The organic layer was washed with brine, dried over sodium sulphate and concentrated *in vacuo*. The residue was purified by column chromatography on silica gel (eluent: 10% ethyl acetate–chloroform) to give **3** (502.0 mg, 68%) as a pale yellow solid. m.p. 217–219°C (decomp.); IR (KBr) 3355, 3291, 3010, 2981, 2918, 2864, 1727, 1613, 1484, 1373, 1225, 1043, 865 cm^{-1}; ^1H NMR (300 MHz, $CDCl_3$) $\delta = 6.98$ (s, 2H), 6.95 (s, 4H), 6.57 (s, 4H), 3.40–4.00 (br, 10H), 2.23 (s, 6H), 2.22 (s, 3H); ^{13}C NMR (150 MHz, $CDCl_3$) $\delta = 148.03$, 147.96, 143.0, 140.1, 130.5, 130.4, 129.6, 127.5, 126.5, 126.4, 116.2, 31.5, 20.4. HR-MS [FAB$^+$] calcd for $C_{38}H_{38}N_2O_5$ 602.2781, found 602.2770 $[M]^+$.

5,17-Bis-[[-2-[[(1,1-dimethylethoxy)carbonyl]amino]-4-methyl-1-oxopentyl]amino]-11,23,29-tri-methyl-31,32,33,34,35-pentahydroxy-calix[5]arene 4

To a solution of calix[5]arene **5** (118.0 mg, 0.196 mmol), *N*-Boc-L-Leu-OH (92.5 mg, 0.400 mmol) and HOAt (55.0 mg, 0.04 mmol) in dichloromethane (15 ml) was added EDCI (82.0 mg, 0.40 mmol). After being stirred at room temperature for 3 h, the reaction mixture was poured into aqueous sodium bicarbonate and the aqueous layer was extracted with dichloromethane. The organic layer was washed with brine, dried over sodium sulphate and concentrated *in vacuo*. The residue was purified by column chromatography on silica gel (eluent: 2% methanol–chloroform) to give **3** (75.4 mg, 38%) as a white solid. m.p. 233–235°C (decomp.); $[\alpha]_D^{25} = -35.1°$ ($c = 0.500$, $CHCl_3$); IR (KBr) 3310, 2958, 2870, 1692, 1621, 1484, 1367, 1287, 1227, 1167, 1047 cm^{-1}; UV–vis ($CHCl_3$) λ_{max} (ε) 254 nm (2.34×10^4), 284 nm (1.62×10^4); ^1H NMR (600 MHz, $CDCl_3$) $\delta = 8.90$ (s, 2H), 8.74 (s, 1H), 8.72 (s, 1H), 8.04 (br s, 1H), 7.36 (s, 4H), 6.98 (s, 6H), 4.87 (s, 2H), 4.20 (s, 2H), 3.30–4.40 (m, 10H), 2.22 (s, 6H), 2.20 (s, 3H), 1.77 (m, 4H), 1.44 (s, 18H), 0.96 (br, 12H); ^{13}C NMR (150 MHz, $CDCl_3$) $\delta = 171.0$, 156.4, 147.8, 147.6, 146.8, 131.4, 130.6, 129.8, 126.9, 126.4, 126.0, 125.9, 121.0, 80.4, 53.7, 41.0, 31.3, 28.3, 24.7, 23.0, 21.7, 20.4. HR-MS [FAB$^+$] calcd for $C_{60}H_{76}N_4O_{11}Na$ 1051.5408, found 1051.5419 $[M + Na]^+$. Anal. calcd for $C_{60}H_{76}N_4O_{11}CH_2Cl_2$: C 65.76, H 7.06, N 5.03; found: C 65.94, H 7.20, N 4.78.

5,17-Bis-[[2-amino-4-methyl-1-oxopentyl]amino]-11,23,29-trimethyl-31,32,33,34,35-pentahydroxy-calix[5]arene bis(hydrotrifluoroacetate) 5

Trifluoroacetic acid (0.30 ml) was added to a solution of **3** (67.1 mg, 0.064 mmol) in dichloromethane (3.0 ml). After being stirred at room temperature for an hour, the reaction mixture was concentrated *in vacuo* to afford the calix[5]arene bis(hydrotrifluoroacetate) (59.0 mg, 86%). ^1H NMR (500 MHz, CD_3OD) $\delta = 7.42$ (s, 2H), 7.41 (s, 4H), 6.98 (s, 2H), 6.96 (s, 4H), 3.95 (m, 2H), 3.84 (s, 4H), 3.82 (s, 4H), 3.78 (s, 2H), 2.18 (s, 9H), 1.75 (m, 4H), 1.01 (d, 6H, $J = 7.0$ Hz), 1.00 (d, 6H, $J = 7.0$ Hz); ^{13}C NMR (125 MHz, CD_3OD) $\delta = 168.7$, 149.6, 149.4, 149.1, 131.9, 131.3, 130.8x2, 130.6, 129.5x2, 128.7, 128.4, 128.2, 122.4, 53.6, 41.7, 31.9, 25.5, 23.1, 22.0, 20.6. HR-MS [FAB$^+$] calcd for $C_{50}H_{61}N_4O_7$ 829.4540, found 829.4533 $[M - 2XCF_3COO^- - H]^+$.

Calix[5]arene-based Receptor 1

A solution of **4** (40 mg, 0.038 mmol) and **5** (35.0 mg, 0.038 mmol) in dimethylformamide (10 ml) was added dropwise to a solution of diisopropylethylamine (0.1 ml) in dimethylformamide (20 ml) at 80°C for 24 h. The reaction mixture was concentrated *in vacuo* and the residue was diluted with ethyl acetate. The organic layer was washed with brine, dried over sodium sulphate and concentrated *in vacuo*. The residue was purified by column chromatography on silica gel (eluent: 2% methanol–chloroform) to give **1** (16.7 mg, 32%) as a white solid. m.p. 221–224°C (decomp.); $[\alpha]_D^{25} = +30.9°$ ($c = 0.502$, $CHCl_3$); IR (KBr) 3319, 2933, 2862, 1656, 1530, 1483,

1322, 1283, 1237, 1146 cm^{-1}; UV–vis ($CHCl_3$) λ_{max} (ε) 252 nm (2.85×10^4); ^1H NMR (600 MHz, $CDCl_3$) $\delta = 8.97$ (s, 1H), 8.90 (s, 1H), 8.78 (s, 1H), 8.64 (s, 2H), 8.49 (s, 2H), 8.42 (s, 1H), 8.25 (s, 1H), 8.21 (s, 1H), 8.09 (s, 1H), 7.96 (s, 1H), 7.70 (s, 1H), 7.64 (d, 1H, $J = 6.2$ Hz), 7.51 (s, 1H), 7.49 (s, 1H), 7.36 (br s, 1H), 7.09 (s, 1H), 7.01 (s, 1H), 7.00 (s, 2H), 6.93 (s, 1H), 6.91 (s, 1H), 6.90 (s, 1H), 6.76 (d, 1H, $J = 8.2$ Hz), 6.57 (d, 1H, $J = 8.2$ Hz), 6.54 (s, 1H), 6.41 (d, 1H, $J = 9.5$ Hz), 6.39 (d, 1H, $J = 9.6$ Hz), 4.80 (m, 1H), 4.79 (m, 1H), 4.37 (q, 1H, $J = 9.6$ Hz), 4.29 (m, 1H), 4.08 (d, 1H, $J = 14.4$ Hz), 4.07 (d, 1H, $J = 13.0$ Hz), 4.05 (d, 1H, $J = 14.5$ Hz), 4.02 (d, 2H, $J = 15.8$ Hz), 3.74 (m, 1H), 3.64 (m, 1H), 3.45 (d, 1H, $J = 13.0$ Hz), 3.41 (d, 1H, $J = 14.4$ Hz), 3.38 (d, 2H, $J = 15.8$ Hz), 3.31 (d, 1H, $J = 14.5$ Hz), 2.33 (m, 2H), 2.29 (s, 3H), 2.27 (s, 3H), 2.26 (s, 3H), 2.14 (m, 4H), 2.05 (m, 2H), 1.94 (m, 2H), 1.86 (m, 2H), 1.75 (m, 1H), 1.69 (m, 1H), 1.57–1.30 (m, 8H), 0.97 (m, 6H), 0.94 (m, 6H); ^{13}C NMR (150 MHz, $CDCl_3$) $\delta = 169.5$, 169.0, 167.1, 166.8, 166.1, 165.2, 164.4, 164.0, 147.9, 147.8, 147.7, 146.9, 146.8, 134.6, 134.5, 133.7, 133.5, 131.2, 130.9, 130.6, 130.3, 130.0, 129.8, 128.9, 127.6, 127.5, 127.2, 126.9, 126.5, 126.3, 125.9, 125.8, 125.5, 121.6, 121.2, 120.4, 58.2, 57.9, 57.2, 52.9, 52.5, 52.4, 52.2, 40.1, 39.1, 32.5, 32.3, 31.9, 31.5, 31.2, 30.9, 29.6, 25.0, 24.8, 24.6, 24.4, 24.1, 22.8, 21.9, 21.8, 20.6, 20.4, 20.3, 18.4. HR-MS [FAB^+] calcd for $C_{80}H_{89}N_8O_{13}$ 1369.6549, found 1369.6515 $[M + H]^+$. Anal. calcd for $C_{80}H_{88}N_8O_{13}\cdot 8.5H_2O$: C 63.10, H 6.95, N 7.36; found: C 63.14, H 6.55, N 7.60.

Acknowledgements

This work was supported by a Grant-in-Aid for Scientific Researches (B) and in Priority Area 'Super-Hierarchical Structures' from the Ministry of Education, Culture, Sports, Science, and Technology, Japan. We are grateful to the Inamori, Kurata and Ogasawara Foundations for financial support.

References

[1] Branden, C.; Tooze, J. *Introduction to Protein Structure*; Garland Publishing: New York, 1992.

[2] Cram, D. J., Cram, J. M., Eds.; *Container Molecules and Their Guests*; 1997; Gokel, G. W.; Ed., *Crown Ethers and Cryptands*, 1991. Lehn, J. M. Ed. *Supramolecular Chemistry: Concepts and Perspectives*, 1995.

[3] Timko, J. M.; Helgeson, R. C.; Cram, D. J. J. *Am. Chem. Soc.* **1978**, *100*, 2828. Peacock, S. S.; Walba, D. M.; Gaeta, F. C. A.; Helgeson, R. C.; Cram, D. J. *J. Am. Chem. Soc.* **1980**, *102*, 2043. Naemura, K.; Miyabe, H.; Shingai, Y.; Tobe, Y. *J. Chem. Soc. Perkin Trans.* **1993**, 1, 1073. Hirose, K.; Ogasahara, K.; Nishioka, K.; Tobe, Y.; Naemura, K. *J. Chem. Soc. Perkin Trans.* **2000**, *2*, 1984. Bradshaw, J. S.; Huszthy, P.; McDaniel, C. W.; Zhu, C. Y.; Dalley, N. K.; Izatt, R. M.; Lifson, S. *J. Org. Chem.* **1990**, *55*, 3129.

[4] Galan, A.; Andreu, D.; Echavarren, A. M.; Prados, P.; de Mendoza, J. J. *Am. Chem. Soc.* **1992**, *114*, 1511.

[5] Erickson, S. D.; Simon, J. A.; Still, W. C. *J. Org. Chem.* **1993**, *58*, 1305, Yoon, S. S.; Still, W. C. *Tetrahedron Lett.* **1994**, *35*, 2117.

[6] Kim, S. -G.; Kim, K. -H.; Jung, J.; Shin, S. K.; Ahn, K. H. *J. Am. Chem. Soc.* **2002**, *124*, 591, Kim, J.; Kim, S.-G.; Seong, H. R.; Ahn, K. H. *J. Org. Chem.* **2005**, *70*, 7227.

[7] Prins, L. J.; Huskens, J.; De Jong, F.; Timmerman, P.; Reinhoudt, D. N. *Nature (London)* **1999**, *398*, 498. Prins, L. J.; Jolliffe, K. A.; Hulst, R.; Timmerman, P.; Reinhoudt, D. N. *J. Am. Chem. Soc.* **2000**, *122*, 3617. Ishi-i, T.; Crego-Calama, M.; Timmerman, P.; Reinhoudt, D. N.; Shinkai, S. *J. Am. Chem. Soc.* **2002**, *124*, 14631. Lazzarotto, M.; Sansone, F.; Baldini, L.; Casnati, A.; Cozzini, P.; Ungaro, R. *Eur. J. Org. Chem.* **2001**, 595. Yakovenko, A. V.; Boyko, V. I.; Kalchenko, V. I.; Baldini, L.; Casnati, A.; Sansone, F.; Ungaro, R. *J. Org. Chem.* **2007**, *72*, 3223. Okada, Y.; Kasai, Y.; Nishimura, J. *Tetrahedron Lett.* **1995**, *36*, 555.

[8] Haino, T.; Yanase, M.; Fukazawa, Y. *Angew. Chem. Int. Ed.* **1998**, *37*, 997. Haino, T.; Nitta, K.; Saijo, Y.; Matsumura, K.; Hirakata, M.; Fukazawa, Y. *Tetrahedron Lett.* **1999**, *40*, 6301. Haino, T.; Araki, H.; Fujiwara, Y.; Tanimoto, Y.; Fukazawa, Y. *Chem. Commun.* **2002**, 2148. Haino, T.; Yamanaka, Y.; Araki, H.; Fukazawa, Y. *Chem. Commun.* **2002**, 402. Haino, T.; Matsumoto, Y.; Fukazawa, Y. *J. Am. Chem. Soc.* **2005**, *127*, 8936. Haino, T.; Seyama, J.; Fukunaga, C.; Murata, Y.; Komatsu, K.; Fukazawa, Y. *Bull. Chem. Soc. Jpn.* **2005**, *78*, 768. Haino, T.; Yanase, M.; Fukazawa, Y. *Tetrahedron Lett.* **2005**, *46*, 1411. Haino, T.; Fukunaga, C.; Fukazawa, Y. *Org. Lett.* **2006**, *8*, 3545. Haino, T.; Yanase, M.; Fukunaga, C.; Fukazawa, Y. *Tetrahedron* **2006**, *62*, 2025. Haino, T.; Fukunaga, C.; Fukazawa, Y. *J. Nanosci. Nanotech.* **2007**, *7*, 1386.

[9] Yoon, S. S.; Still, W. C. *Tetrahedron* **1995**, *51*, 567.

[10] Haino, T.; Harano, T.; Matsumura, K.; Fukazawa, Y. *Tetrahedron Lett.* **1995**, *36*, 5793. Haino, T.; Yanase, M.; Fukazawa, Y. *Tetrahedron Lett.* **1997**, *38*, 3739. Haino, T.; Yanase, M.; Fukazawa, Y. *Angew. Chem., Int. Ed. Engl.* **1997**, *36*, 259. Haino, T.; Matsumura, K.; Harano, T.; Yamada, K.; Saijyo, Y.; Fukazawa, Y. *Tetrahedron* **1998**, *54*, 12185.

[11] Iwamoto, H.; Yukimasa, Y.; Fukazawa, Y. *Tetrahedron Lett.* **2002**, *43*, 8191.

[12] Böhmer, V.; Dalla Cort, A.; Mandolini, L. *J. Org. Chem.* **2001**, *66*, 1900.

[13] Mohamadi, F.; Richards, N. G. J.; Guida, W. C.; Liskamp, R.; Lipton, M.; Caufield, C.; Chang, G.; Hendrickson, T.; Still, W. C. *J. Comput. Chem.* **1990**, *11*, 440. Reddy, M. R.; Erion, M. D.; Agarwal, A.; Viswanadhan, V. N.; McDonald, D. Q.; Still, W. C. *J. Comput. Chem.* **1998**, *19*, 769.

[14] Inoue, Y.; Hakushi, T. *J. Chem. Soc. Perkin Trans.* **1985**, *2*, 935. Inoue, Y.; Amano, F.; Okada, N.; Inada, H.; Ouchi, M.; Tai, A.; Hakushi, T.; Lu, Y.; Tong, L.-H. *J. Chem. Soc. Perkin Trans.* **1990**, *2*, 1239. Smithrud, D. B.; Wyman, T. B.; Diederich, F. *J. Am. Chem. Soc.* **1991**, *113*, 5420.

[15] Haino, T.; Kobayashi, M.; Fukazawa, Y. *Chem. Eur. J.* **2006**, *12*, 3310. Tokunaga, Y.; Rudkevich, D. M.; Rebek, Jr., J. *Angew. Chem. Int. Ed. Engl.* **1997**, *36*, 2656. Kang, J.; Rebek, Jr., J. *Nature* **1996**, *382*, 239. Grotzfeld, R. M.; Branda, N.; Rebek, Jr., J. *Science* **1996**, *271*, 487.